BUILDING RESPONSE ANALYSIS AND DAMAGE DETECTION USING SUBSPACE IDENTIFICATION METHODS

Kenneth J. Loh and Chin-Hsiung Loh

Department of Structural Engineering
University of California, San Diego

Abstract

The overarching goal of this research is to derive innovative methodologies for analyzing diverse sensing streams to yield actionable information that directly support post-earthquake response, emergency management, and disaster recovery. As a step towards this goal, the objective of this study is to use data collected from the California Strong Motion Instrumentation Program (CSMIP) to demonstrate that a particular class of system identification (SI) techniques – namely, subspace identification (SI) or recursive subspace identification (RSI) – is especially suitable for rapid, post-disaster, structural health assessment. The advantage of SI/RSI is that it is an input-output and data-driven method, where only structural response records (*e.g.*, acceleration records) are needed for extracting dynamic properties of the structure. In this paper, both SI and RSI were be applied to assess CSMIP-instrumented buildings with acceleration records from past ground motion events. The result verified that building dynamic characteristics (*i.e.*, natural frequencies and mode shapes) could be clearly identified using all the recorded data simultaneously. In addition, the RSI algorithm was also employed for analyzing data recorded from the Northridge earthquake event. Time-varying modal properties of the building were also examined.

Introduction

Strong motion data acquired from structures during seismic events can play a vital role in gaining insights into the behavior of these systems if a systematic procedure is adopted in analyzing the acquired data. This process, known as system identification (ID), is an inverse problem in structural dynamics that involves the determination of mathematical models and the estimation of structural parameters based on measured responses under known excitations. Several methods, from the simple transfer function to the more sophisticated output error methods, have been devised [1]. In general, two different approaches have been used to assess the behavior of structures (*i.e.*, most commonly bridges) from their recorded data. The first approach is to develop a finite element model (FEM) and to modify the FEM parameters to match the measured response. This approach looks very attractive but has a major pitfall, since the FEM parameters have to be updated by a trial-and-error process. The second approach is to identify the modal parameters of the system and to study the changes in the structural dynamic characteristics. In this study, the inverse problem (*i.e.*, identification of the system state) will be used.

Many offline system identification algorithms that can be implemented for time-invariant systems with constant modal parameters were developed in the past (*e.g.*, the Kalman filter technique, Eigensystem realization algorithm (ERA) [2], and autoregressive exogenous (ARX) model [3]). Over the past few years, various system ID algorithms have been successfully applied, many of which uses both input and output data [4-7]. Several well-known offline system ID algorithms, including canonical variable analysis (CVA), numerical algorithms for subspace state space system identification (N4SID), multivariable output-error state space algorithm (MOESP), and Instrumental Variable-subspace state space system identification (IV-4SID) [8-10], have been developed.

Traditional system ID algorithms for analyzing building seismic response data and extracting system dynamic characteristics have predominantly been based on multi-input multi-output (MIMO) ARX models. However, they do suffer from several disadvantages:

- It is difficult to determine the model order of multivariate ARX model, and further optimization of parameters needs to be performed.
- There are too many unknown parameters to be estimated, where convergence in optimization may take time and require significant computational effort.
- While it is easy to estimate the frequency response function (FRF) between each pair of response measurements, but it is difficult to estimate the system mode shapes and natural frequencies.

Therefore, in this study, the subspace identification (SI) algorithm was used to analyze the seismic response data of two buildings, namely, the seven-story Van Nuys building and the 13-story Sherman Oaks building. The objective was to examine the dynamic characteristics of these buildings when they were subjected to different earthquake excitations. Furthermore, the recursive subspace identification (RSI) algorithm was also applied to the data collected from these two buildings during the Northridge earthquake. Unlike conventional system ID, SI has the following advantages:

- A good initial model can be quickly obtained with subspace methods, since the linear state space model is employed.
- SI provides simple parametrization for MIMO systems as well as robust noniterative numerical solutions.
- The reliable numerical tool-based methods, such as LQ decomposotion and singular value decomposition (SVD), are employed in the algorithm.
- SI provides rapid adoption in application through the use of stabilization diagrams to reliably estimate system dynamic characteristics.

Subspace Identification using Both Input and Output Measurements

In this section, data-driven subspace identification (SI-DATA) was used to extract the system dynamic characteristics seismic response data of the structure. First, consider a discrete time, state-space, dynamic system with n degree-of-freedoms (DOF). The system equation can be represented as [9]:

$$\mathbf{X}_{k+1} = \mathbf{A}_d\mathbf{X}_k + \mathbf{B}_d\mathbf{u}_k + \mathbf{w}_k \quad (1a)$$

$$\mathbf{y}_k = \mathbf{C}_c\mathbf{X}_k + \mathbf{D}_c\mathbf{u}_k + \mathbf{v}_k \quad (1b)$$

with $\mathbf{A}_d = \exp(\mathbf{A}_c \Delta t) \in \mathbb{R}^{2n \times 2n}$, $\mathbf{B}_d = (\mathbf{A}_d - \mathbf{I}_{2n})\mathbf{A}_c^{-1}\mathbf{B}_c \in \mathbb{R}^{2n \times m}$. $\mathbf{A}_d$ is called the discrete-time state matrix, $\mathbf{B}_d$ is the discrete-time input matrix, $\mathbf{X}_k = \mathbf{X}(k\Delta t)$ is the discrete-time state vector, Δt is the sample time, and $k \in \mathbb{N}$. Here, $\mathbf{w}_k \in \mathbb{R}^{2n \times 1}$ is the process noise due to disturbances or modeling error, and $\mathbf{v}_k \in \mathbb{R}^{l \times 1}$ is the measurement noise due to disturbances or malfunction of the sensing nodes. Equation 1 is also known as a discrete-time combined deterministic-stochastic system, because it is a combination of a deterministic system and a stochastic system by combining the state $\mathbf{X}_k$ and output $\mathbf{y}_k$ individually. For subspace identification, the input and output measurements should be arranged into the format of a "data Hankel matrix". If the modal properties (*i.e.*, natural frequency, damping ratio, and mode shape) of the structure are needed, the Multivariable Output-Error State Space algorithm (MOESP) can be employed to extract the column space of the extended observability matrix from the LQ decomposition of the Hankel matrix [10].

Implementation of the Stabilization Diagram for SI

When applying SI-DATA for structural system identification, the method does not yield exact values for the parameters but only estimates with uncertainties. These uncertainties are responsible for the appearance of spurious modes. One of the important challenges is to remove these spurious modes. For this purpose, the stabilization diagram is used. The stabilization diagram has frequencies plotted in the horizontal axis and model orders plotted in the vertical axis. The quality of the stabilization diagram depends on the values of the input parameters of the algorithm and the noise ratio of the time series under analysis. In order to present a better visualization using stabilization diagram, certain criteria to remove the spurious modes need to be defined. In this study, four criteria were used and are described next.

First, the duration of the recorded data was selected. Since the seismic response data collected from the structure may contain pre-event memory data as well as the coda wave, therefore, the criterion to select the duration of data for SI must be defined. The initial time from the recorded data can be determined from the concept of a P-wave picker by using the following equation for calculating the Arias Intensity Criterion (AIC) [12]:

$$AIC(t) = t\log(\mathrm{var}(a[1:t])) + (N - t + 1)\log(\mathrm{var}(a[t+1:N])) \tag{2}$$

where t is the time moving window length, and N is entire time length. In addition, var(a[1:t]) is the variance of the data *a(t)*. The initial starting time can be determined from the time when the rate of slope of AIC values change dramatically, as is shown in Figure 1 and corresponding to when t is 15.0 s. Besides, the end point of the data can be determined from the plot of Arias Intensity when it reaches 99.5% (also shown in Figure 1 and when t is 56.5 s).

Second, depending on the quality of the data, a low-pass filter may be applied. Here, a Butterworth filter with order 10 was employed to filter out the high frequency signals so as to enhance the quality of the stabilization diagram. Third, for each model order, the identified mode shapes of the structure was identified. To ensure that these were the correct mode shapes, the modal assurance criterion (MAC) was applied between two different model orders:

$$MAC(\Phi^*_j \cdot \Phi_i) = \frac{\left|\Phi^*_j \cdot \Phi_i\right|^2}{(\Phi^*_j \cdot \Phi_j)(\Phi^*_i \cdot \Phi_i)} \geq MAC_\phi \tag{3}$$

The value of $MAC(\Phi^*_j \cdot \Phi_i)$ is a user-defined value (*e.g.*, by setting the threshold to 95%).

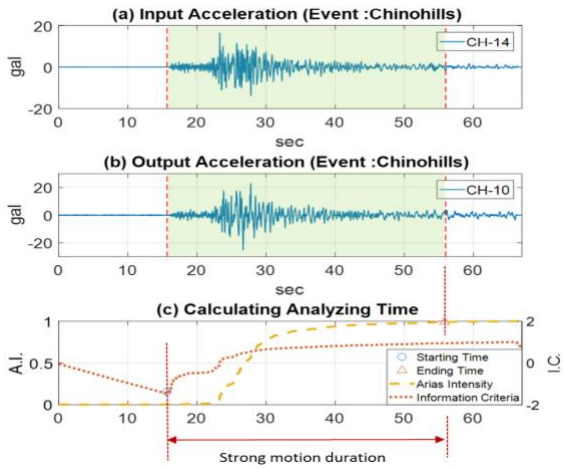

Figure 1. Plot of AIC and normalized Arias intensity to identify the strong motion duration

Last, the modal phase collinearity (MPC) could be calculated. For each particular identified mode, it was necessary to check the phase collinearity among each measurement node. The phase vector Ψ_k of a *kth* mode from *l* measurement nodes is shown as:

$$\text{phase}(\boldsymbol{\psi}_k) = [b_{k,1} \quad b_{k,2} \quad \cdots \quad b_{k,l}]^T \in \mathbb{R}^{l\times 1} \quad (-\pi \le b < \pi) \tag{4}$$

To ensure that it is the correctly identified mode, the phase difference among each measurement node should be either in-phase or out-of-phase:

$$|b_{k,q} - b_{k,r}| = 0 \quad \text{or} \quad \pi \quad (q \ne r) \tag{5}$$

Figure 2 shows an example of a stabilization diagram that compares different criteria applied. For all cases, a low-pass filter with a cutoff frequency of 50 Hz was implemented. In general, it can be observed that the consideration of both criteria (*i.e.*, MAC of 0.95 and MPC of 0.90) resulted in clear modes being identified (*i.e.*, green circles in Figure 2). Besides, with increasing model order, more noise modes can be observed.

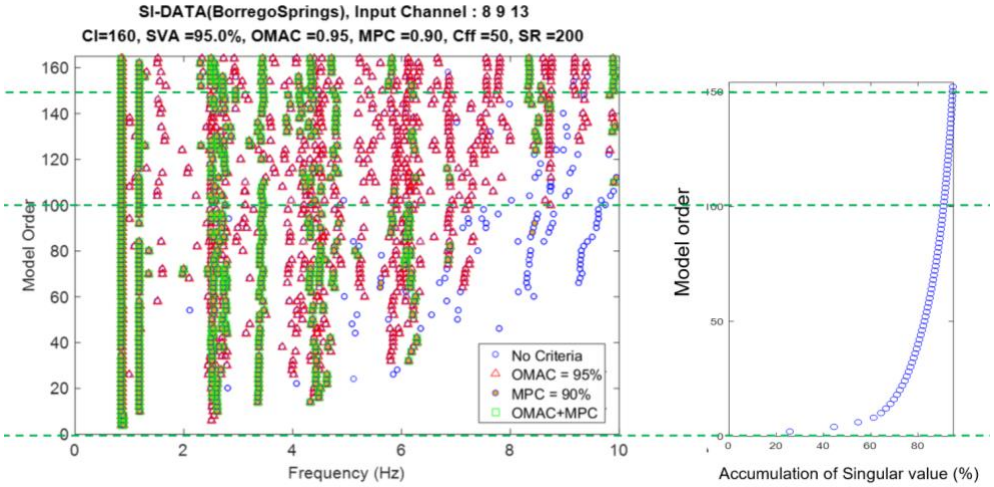

Figure 2. Example of a stabilization diagram with different criteria applied to remove spurious modes.

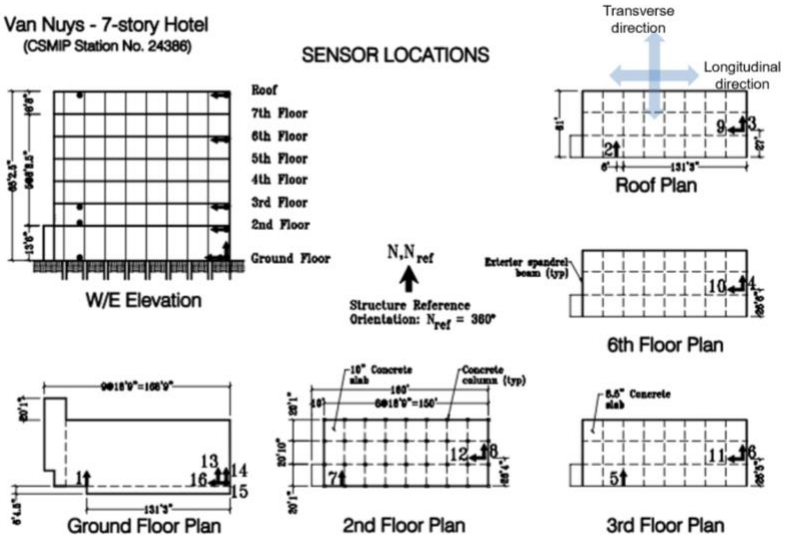

Figure 3. Layout of strong motion instrumentation in the 7-story Van Nuys building.

Table 1: List of earthquake event from Van Nuys building for analysis.

Date	Earthquake	Epic.(Fault) Dist.(km)	Peak Acceleration (g)		Data
			Ground	Struct.	Raw data
1994/6/17	Northridge #	7.0 (1.7)	0.47	0.59	V(broken)
2008/7/29	Chinohills #	71.5 (--)	0.054	0.14	v(missing CH:8,13)
2010/7/7	BorregoSprings #	203.8 (--)	0.004	0.016	V(Missing CH:8,13)
2014/3/17	Encino #	9.8 (--)	0.144	0.219	v(Missing CH:8,13)

Building Seismic Response Analysis using SI-DATA

Analysis of the 7-Story Van Nuys Building

The Van Nuys building was instrumented with 16 accelerometers in 1980 and by CSMIP. Figure 3 shows the instrument layout in the building with 16 accelerometers distributed across five levels. The building was repaired and strengthened with concrete shear walls after the 1994 Northridge earthquake. Among all the seismic event recorded from the building, four seismic events (as shown in Table 1) were selected for the analysis conducted in this study. Prior to SI analysis, the time-frequency analysis on the roof response data of the building was generated. The modified complex Morlet wavelet with variable central frequency was used to generate the spectrogram [14]. Figure 4a shows the spectrograms calculated using Channels 9 and 3 of the Northridge earthquake data, while Figure 4b shows the spectrograms for the Encino earthquake data; all these channels corresponded to the roof response data. A comparison between these two sets of event data shows a significant change in the fundamental dominant frequency from about 0.5 Hz to 2.0 Hz. This result is expected and is consistent with the retrofit performed after the Nothridge earthquake, which would increase the stiffness of the structure and hence its dominant frequency.

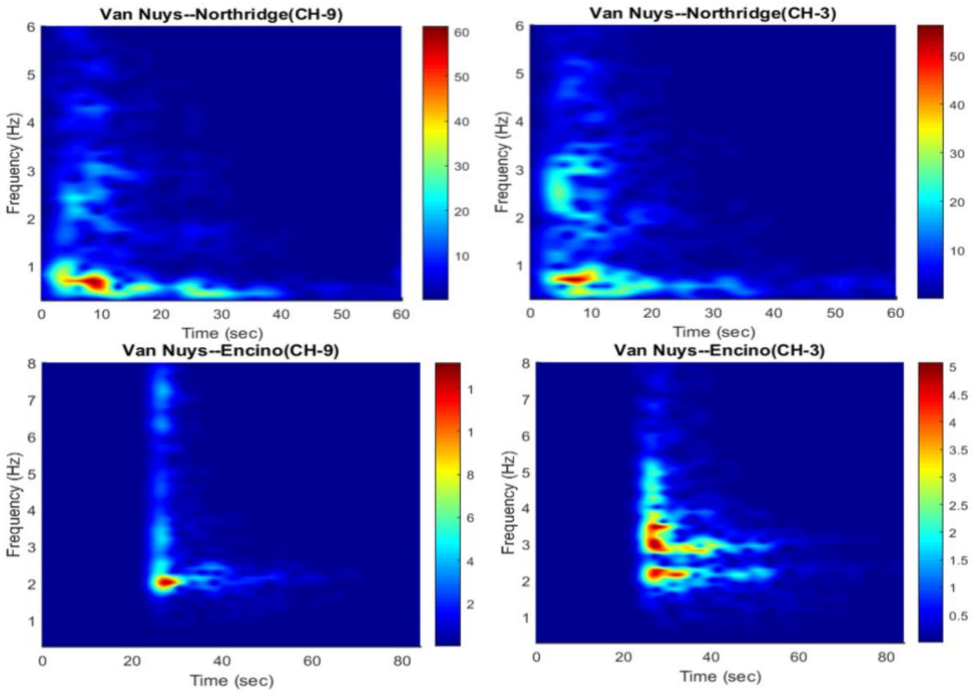

Figure 4. Spectrograms of Channels 3 and 9 of the Van Nuys building corresponding to two seismic events: (top) Northridge earthquake and (bottom) Encino earthquake

Before using SI to determine the dynamic characteristics of the Van Nuys building, the sensitivity of model order according to the stabilization diagrams was examined. Figure 5 shows two stabilization diagrams computed using two different model orders (*i.e.*, based on *cl* values 120 and 160) corresponding to the Northridge earthquake data. Since a larger model order would include more data in each column of the data Hankel matrix, more noisy modes would appear. However, at the same time, a larger model order also means that some extra modes could be identified. For the case of the Northridge earthquake dataset, one could identify the torsional mode at frequency of 0.697 Hz. This mode can not be observed for the case when the *cl* value was set to 120. Using the spectrogram corresponding to a *cl* value of 160, three fundamental modes from the Northridge earthquake record was constructed, as is shown in Figure 6. The first mode is the longitudinal mode, the second mode is a combination of longitudinal and transverse modes, and the third mode is the torsional mode.

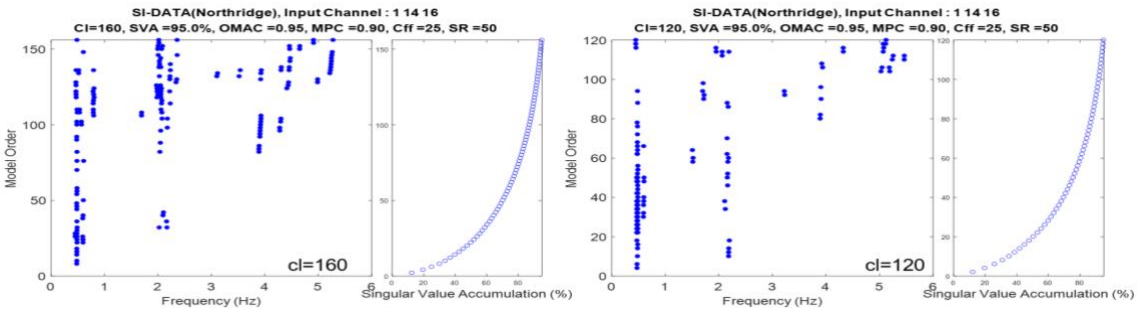

Figure 5. Comparison of stabilization diagrams using two different *cl* values.

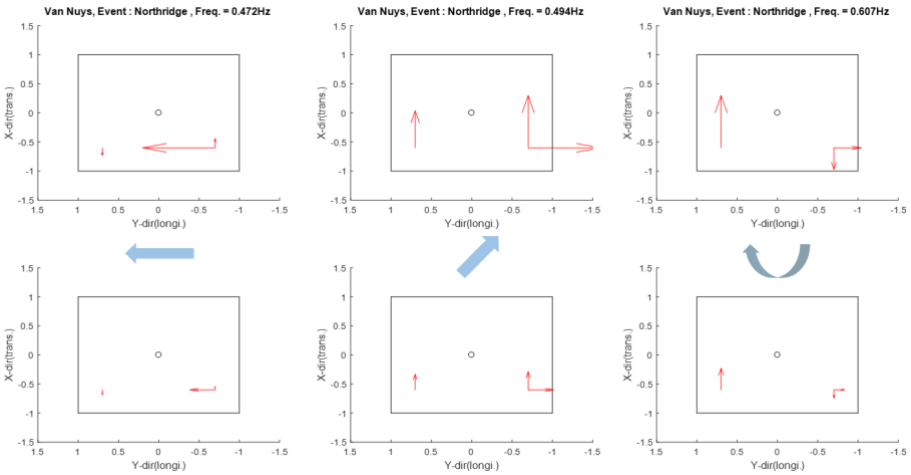

Figure 6. The three fundamental modes of the Van Nuys building was identified using SI (corresponding to data from the Northridge earthquake).

A similar approach was also employed for the other three earthquake events selected for this study. Figure 7 shows the stabilization diagrams from the other three small earthquake event datasets. It can be observed that the identified dominant frequencies are quite consistent among these events. Table 2 shows the comparison of the three identified fundamental frequencies of the building. Furthermore, the differences of these modal frequencies with respect to the result from Northridge earthquake is significant. As mentioned earlier, this result is expected and is due to the influence of retrofitting the building after the Northridge earthquake. The identified mode shapes from the Chino Hills earthquake is shown in Figure 8. The major difference observed between the Northridge and Chino Hills event is the second mode. For the small earthquake event, one can identify the transverse mode, while, for the larger Northridge earthquake, the second mode appears to be a combination of longitudinal and transverse motions.

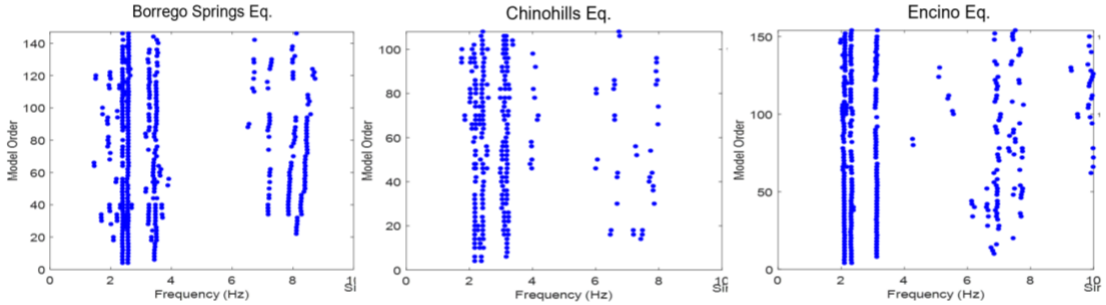

Figure 7. Stabilization diagrams from three earthquake events, namely, the Borrego Spring, Chino Hills, and Encino earthquakes

Table 2. Identified modal frequencies of the Van Nuys building

Event\Mode	1st mode (Longitudinal)	2nd mode (Transverse)	3rd mode (Torsion)
Northridge	0.468	0.487	0.697
Chinohill	2.174	2.382	3.172
BorregoS.	2.388	2.577	3.442
Encino	2.111	2.327	3.133

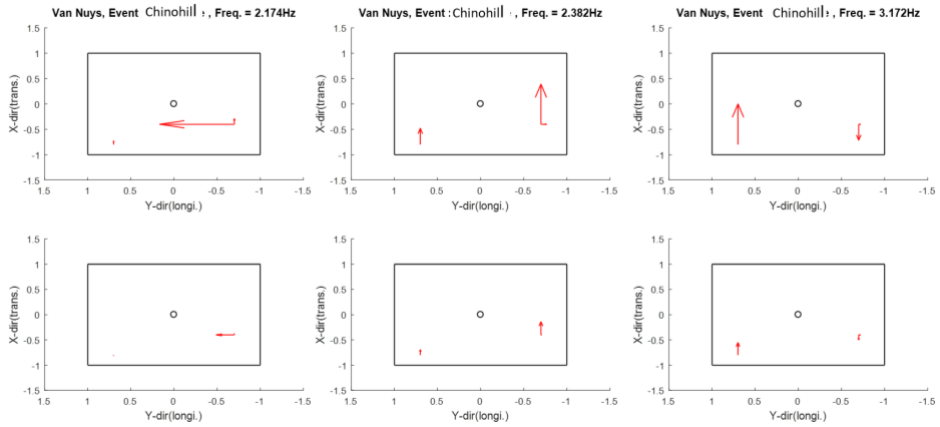

Figure 8. The identified three fundamental modes using data from the Chino Hills earthquake

Analysis of the 13-Story Sherman Oaks Building

In 1977, the 13-story Sherman Oaks building was instrumented with 15 accelerometers across five different levels. This building was also retrofitted with friction dampers after the 1994 Northridge Earthquake. Figure 9 shows the instrument layout in the building. Among all the recorded earthquake events from this building, five event datasets were selected for this study. SI analysis was performed using the same procedure as was described in the previous section and, specifically, for identifying the system natural frequencies.

Figure 10 shows the comparison of the stabilization diagrams corresponding to three different seismic events. It can be observed that the differences among these three stabilization diagrams are quite significant. First, the change in modal frequencies among these three dataset are obvious. One reason is because both the Whittier and Northridge earthquakes induced significant structural response, and this could have caused the structural system to undergo inelastic deformation. Second, the other reason is because the building was retrofitted with friction dampers after the 1994 Northridge earthquake.

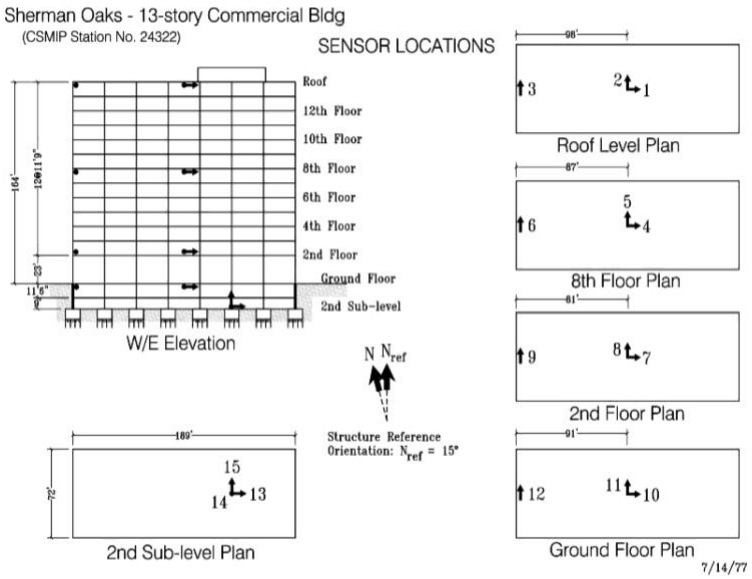

Figure 9. Strong motion instrumentation layout in the 13-story Sherman Oaks building

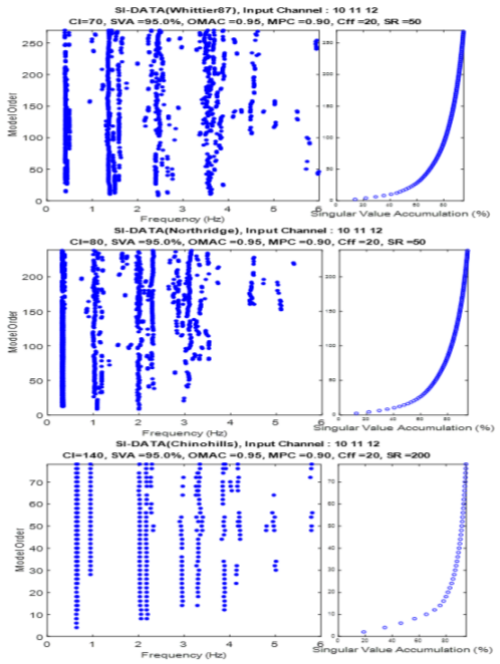

Figure 10. Stabilization diagrams corresponding to three different seismic events (*i.e.*, the Whittier, Northridge, and Chino Hills earthquakes).

Table 3 summarizes the identified natural frequencies of the Sherman Oaks building when SI was performed using five different earthquake datasets. In addition, the identified mode shapes from Whittier, Northridge, and Chino Hills earthquakes are shown in Figure 11. The mode shapes extracted from the two large earthquake excitations are significantly different than the mode shapes identified from the other smaller event datasets.

Table 3. Identified modal frequencies of the Sherman Oaks 13-story building.

Shenman Oak 13-story Building	Horizontal Peak Acceleration (g)		*Identified system natural frequency (Hz)*								
	Groiund	*Structture*	*1st -Trans.*	*1st -Long.*	*2nd -Trans.*	*2nd -Long.*	*3rd -Trans.*	*4th -Trans.*	*1st -Tor.*	*2nd -Tor.*	*3th -Long.*
Whittire87 EQ	0.15	0.17	0.408	0.448	1.368	1.501	2.398	3.534			
Northridge EQ	0.46	0.90	0.327	0.348	1.09		2.001				
Chinohills EQ	0.049	0.094	0.644	0.664	2.034	2.178	3.313		0.952	2.956	3.885
Calexico EQ	0.004	0.02	0.958	0.657	2.08	2.213		3.425	3.036		3.927
Encino EQ	0.242	0.538	0.634	0.656	1.953	2.155		3.23	2.918		3.841

Figure 11. The identified modes shapes of the 13-story Sherman Oaks building using three earthquake event datasets (*i.e.*, Whittier, Northridge, and Chino Hills earthquakes).

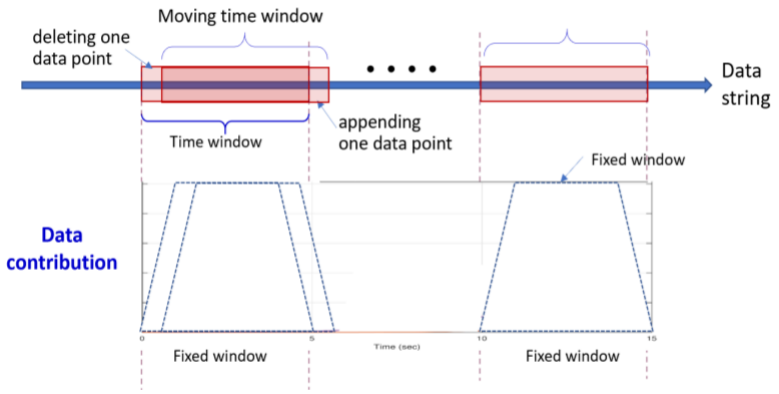

Figure 12. Concept of the moving window used in recursive subspace identification

Recursive Subspace Identification (RSI) with BonaFide LQ Renewing Algorithm

Despite the advantages of the SI-DATA algorithm, a disadvantage is that it is an offline identification technique and that it can only estimate the time-varying state of a structure. In order to track the time-varying modal properties of the system during strong earthquake excitations, recursive (or online) subspace identification needs to be used. The concept of recursive subspace identification is similar to moving time window system ID, as is illustrated in Figure 12. The analysis of the initial time window is the same as that of the SI-DATA algorithm (as was described in the previous section). When a new set of input and output data are appended, the RSI-BonaFide is applied. Furthermore, the RSI-BonaFide-Oblique algorithm is a projection matrix renewing method based on an oblique projection accomplished by LQ decomposition performed on the data Hankel matrix. One of the most significant points about the RSI-BonaFide-Oblique method is that it utilizes a fixed-length moving window technique that keeps the analyzed length of input and output data as a constant; therefore, there is no forgetting factor used in this particular algorithm [15].

Building Response Seismic Analysis using RSI

Since the peak ground acceleration and the peak acceleration response recorded from the 7-story Van Nuys building during Northridge earthquake excitation were 0.47 g and 0.59 g, respectively, it was believed that the building was most likely experienced inelastic response. Thus, the RSI-BonaFide method was used to investigate the time-varying modal parameters of the building. In order to simplify the analysis, instead of using all of the recorded data from the building, only the basement and roof acceleration records in longitudinal and transverse directions were used. The window length was selected and fixed as 4 s, and the duration of the window shift was set as 0.5 s. Figure 13 shows the identified time-varying modal frequencies in the longitudinal and transverse directions. It should be clarified that the result only provides the natural frequencies and their change with respect to time, and there it is not possible to detect the change of stiffness in the structure.

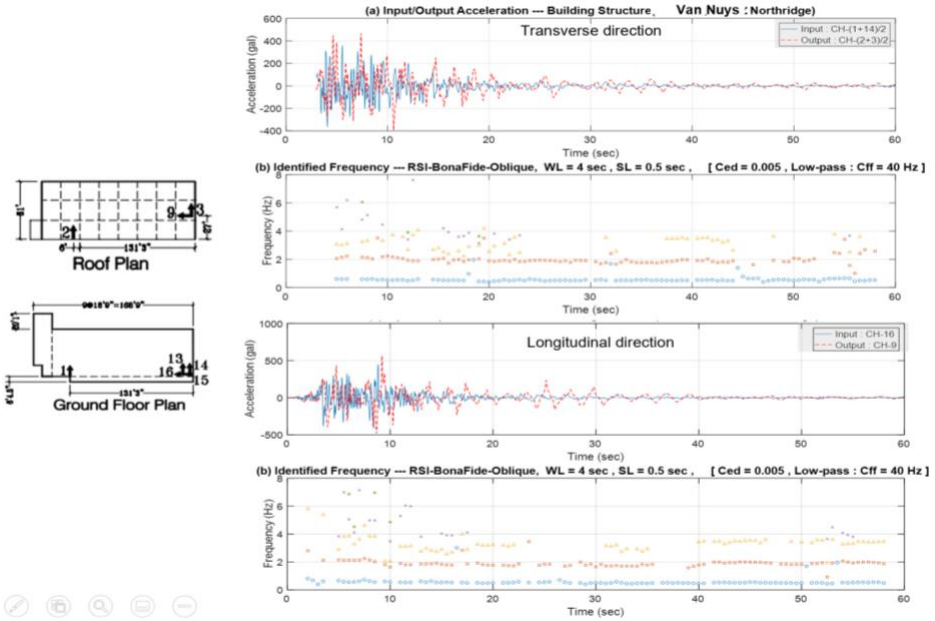

Figure 13. The identified time-varying modal frequencies of the Van Nuys building during the Northridge earthquake as determined using RSI-BonaFide algorithm

According to Caicedo *et al.* [16], a least squares optimization was developed to estimate the inter-story stiffness of each DOF using the identified modal parameters, such as by using the modal frequencies and mode shapes. Consider an *n*-story shear-type structure with one translational DOF on each floor (*i.e.*, 1 DOF per floor). The method was derived from the eigen-equation of this *n*-DOF system (where *n* = 1xN). At each time instant *t* = k s, one can define the eigen-equation of the r_{th} mode according to Equation 6:

$$\mathrm{K}_{System}\Phi_{r,(t=k)} = \omega^2_{r,(t=k)}\mathrm{M}_{System}\Phi_{r,(t=k)} \tag{6}$$

where *r* = 1, 2, 3, …, *s*, and *s* is the number of the identified modes (s ≤ n) from RSI. By assuming that the structural model is a lumped-mass system, the mass and stiffness matrices can be expressed as:

$$\mathrm{M}_{System} = \begin{bmatrix} m_1 & 0 & 0 & 0 \\ 0 & m_2 & 0 & 0 \\ 0 & 0 & \ddots & 0 \\ 0 & 0 & 0 & m_n \end{bmatrix} \tag{7}$$

$$\mathrm{K}_{System} = \begin{bmatrix} k_1 + k_2 & -k_2 & 0 & 0 \\ -k_2 & k_2 + k_3 & \ddots & 0 \\ 0 & \ddots & \ddots & -k_n \\ 0 & 0 & -k_n & k_n \end{bmatrix} \tag{8}$$

It is assumed that the system mass matrix is known *a priori*. Then, the only unknown variables become the inter-story stiffness of each floor, namely $k_1, k_2, \ldots k_n$. At each time instant "k", the equation can be re-organized as shown in Equation (9).

$$\begin{bmatrix} \Delta_1 \\ \Delta_2 \\ \vdots \\ \Delta_s \end{bmatrix}_{(s\times n)\times n} \times \begin{bmatrix} k_1 \\ k_2 \\ k_3 \\ \vdots \\ k_n \end{bmatrix}_{(n\times 1)} = \begin{bmatrix} \Lambda_1 \\ \Lambda_2 \\ \vdots \\ \Lambda_s \end{bmatrix}_{(s\times n)\times 1} \tag{9}$$

The identified mode shapes can then be allocated into a matrix. $\Delta_{(t=k)}$ is allocated with the identified mode shapes with a dimension of $(s \times n) \times n$. The multiplication of modal frequency, mode shape, and floor mass also needs to form a single vector, namely $\Lambda_{(t=k)}$, with a dimension of $(s \times n) \times 1$. It should be mentioned that the number of identified modes is usually less than the number of exact modes in the structural system (*i.e.*, $s \leq n$). Nevertheless, the inter-story stiffness can then be estimated. In general, the result can provide a first stage safety assessment of the building by using the identified time-varying inter-story stiffnesses. Besides, to update the mass and stiffness matrices and make them compatible with both the measured eigenvalues and eigenvectors computed at each time instant, a model updating technique called efficient model correction method (EMCM), proposed by Yuen [17], can be applied.

For detecting the time-varying stiffness of the 7-story Van Nuys during an earthquake, a simplified lumped mass model needs to be assumed. This assumption needs to incorporate the distribution of the instrumented earthquake monitoring system. For simplicity, this building was assumed to be a 2-DOF system with mass $m_1 = 4M$ and $m_2 = 3M$, as is shown in Figure 14. The identified time-varying stiffness (stiffness index) of this 2-DOF simplified model is also shown in Figure 14. It should be mentioned that the variation of the stiffness index with respect to time does not indicate the dramatic change of stiffness at every instant of time during the earthquake excitation. As described earlier, this is the result of an equivalent linear stiffness index (secant stiffness) within the preselected and designated time window. For safety assessment of the structure, one should first apply the same approach to assess the time-varying stiffness of the structure using datasets corresponding to smaller seismic events, where the structure performed linearly. In doing so, the dynamic characteristics of the system can be acquired in a more stable fashion to build up a correct nominal model (*i.e.*, corresponding to the undamaged case). This approach was also applied to the 13-story Sherman Oaks building, and the result is shown in Figure 15.

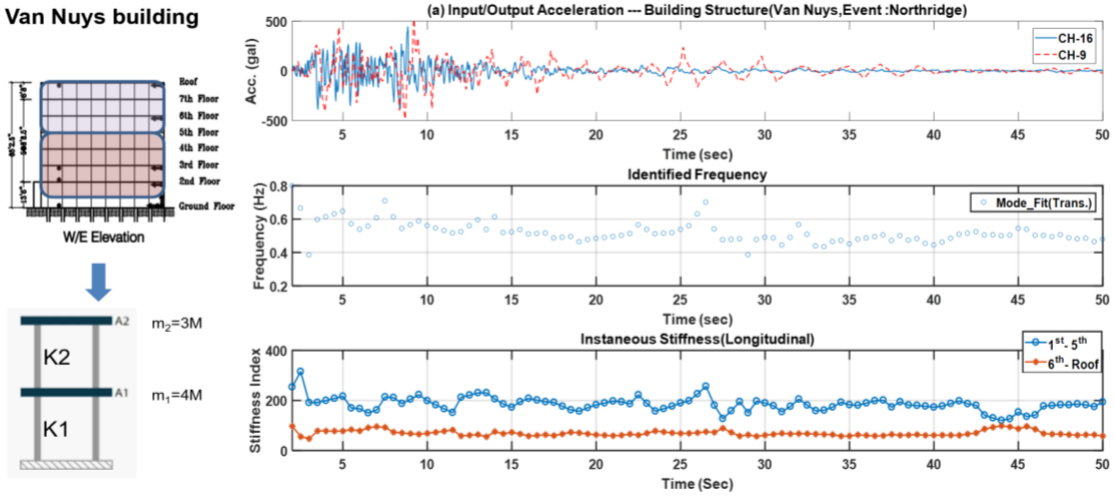

Figure 14. The identified time-varying stiffness index from the simplified model of the 7-story Van Nuys building

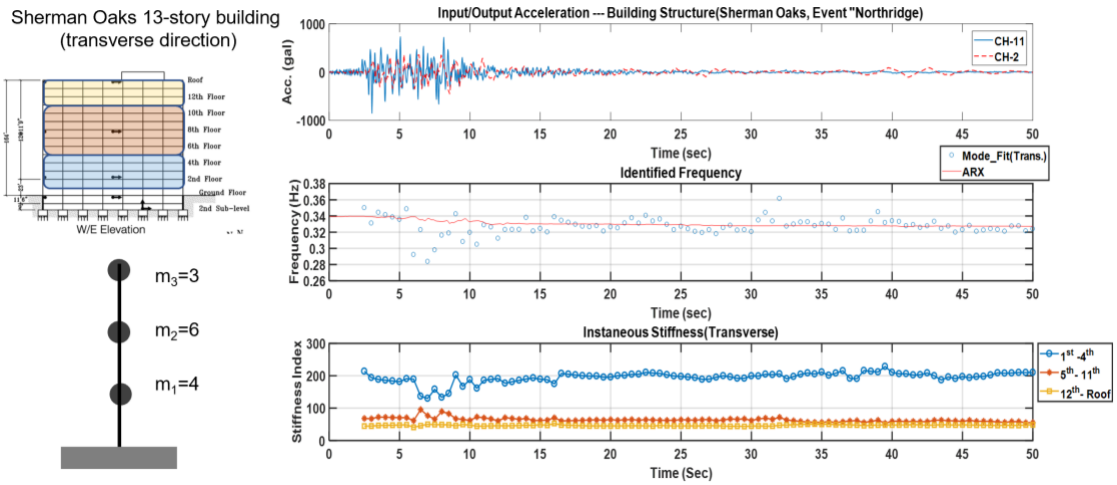

Figure 15. The identified time-varying stiffness index from the simplified model of the 13-story Sherman Oaks building

Conclusions

In this study, both subspace identification and recursive subspace identification with BonaFide LQ renewing algorithm (*i.e.*, incorporating a moving window technique) were utilized to identify the modal parameters (namely the natural frequencies and mode shapes) of two buildings during strong earthquake excitations. For SI, the stabilization diagram played an important role for extracting the real structural modes while removing the spurious modes. For RSI, based on strong seismic response datasets collected from the two buildings (*i.e.*, 7-story Van Nuys and 13-story Sherman Oaks buildings), one could identify their time-varying modal frequencies during these events. The least squares stiffness method was used to estimate the system stiffness matrix using simplified models of these structures. In general, the conclusion was that SI could provide a convenient and systematic multivariate system identification method for estimating the dynamic characteristics of these buildings. By combining the result from RSI (corresponding to when the structure was subjected to strong motion) and by developing a nominal model (corresponding to the undamaged case), one can potentially conduct damage assessment.

Acknowledgments

This research was supported by the Department of Conservation for the California Strong Motion Instrumentation Program (CSMIP) data interpretation project no. 1018-567.

References

[1] C. R. Farrar, S. W. Doebling, and D. A. Nix, 2001, "Vibration-based structural damage identification," *Philosophical Transactions of the Royal Society A*, **359**(1778): 131-149.

[2] J. N. Juang, *Applied System Identification*. Prentice Hall: Upper Saddle River, NJ (1994).

[3] L. Lennart, *System Identification: Theory for the User, 2nd edition*. Prentice Hall: Upper Saddle River, NJ (1999).

[4] B. D. Rao and K. S. Arun, 1992, "Model based processing of signals: a state space

approach," *Proceedings of the IEEE*, **80**(2): 293-309.

[5] A-J. van der Veen, E. F. Deprettere, and A. L. Lee Swindlehurst, 1993, "Subspace based signal analysis using singular value decomposition," *Proceedings of the IEEE*, **81**(9): 1277-1308.

[6] M. Viberg, 1994, "Subspace methods in system identification," *IFAC Proceedings Volumes*, **27**(8): 1-12.

[7] P. van Overschee and B. De Moor, *Subspace Identification for Linear Systems: Theory-Implementation-Applications*. Kluwer Academic Publishers: Dordrecht, Netherlands (1996).

[8] W. E. Larimore, 1994, "The optimality of canonical variate identification by example," *Proceedings of SYSID*, **94**: 151-156.

[9] P. van Overschee and B. De Moor, 1994, "N4SID: Subspace algorithms for the identification of combined deterministic-stochastic systems," *Automatica*, **30**(1): 75-93.

[10] M. Verhaegen, 1994, "Identification of the deterministic part of MIMO state space models given in innovations form from input-output data," *Automatica*, **30**(1): 61-74

[11] J. C. Willems, 1986, "From time series to linear systems, part I," *Automatica*, **22**(5): 561-580.

[12] H. Zhang, C. Thurber, and C. Rowe, 2003, "Automatic p-wave arrival detection and picking with multiscale wavelet analysis for single-component recordings," *Bulletin of the Seismological Society of America*, **93**(5): 1904-1912.

[13] J-H. Weng, C-H. Loh, and J. N. Yang, 2009, "Experimental study of damage detection by data-driven subspace identification and finite-element model updating," *Journal of Structural Engineering*, **135**(12): 1533-1544.

[14] W. Hsueh and C-H. Loh, 2017, "Damage detection of structures by wavelet analysis: application to seismic response of steel frames," *Proceedings of SPIE – Sensors and Smart Structures Technologies for Civil, Mechanical, and Aerospace Systems*, **10168**: 1016811.

[15] K. Kameyama, A. Ohsumi, Y. Matsuura, and K. Sawada, 2005, "Recursive 4SID-based identification algorithm with fixed input-output data size," *International Journal of Innovative Computing, Information and Control*, **1**(1): 17-33.

[16] J. M. Caicedo, S. J. Dyke, and E. A. Johnson, 2004, "Natural excitation technique and eigensystem realization algorithm for phase I of the IASC-ASCE benchmark problem: simulated data," *Journal of Engineering Mechanics*, **130**(1): 49-60.

[17] K. V. Yuen, 2010, "Efficient model correction method with modal measurement," *Journal of Engineering Mechanics*, **136**(1): 91-99.